THE GALACTIC RADIO SPECTRUM DOWN TO 19·7 Mc/s

By M. M. Komesaroff*

[*Manuscript received August* 16, 1961]

Summary

Studies of the galactic radio spectrum have been carried out using results of a number of surveys between 19·7 and 1390 Mc/s. About 4–5° from the equator the spectrum is non-thermal and the temperature spectral index has a constant value of $2 \cdot 6 \pm 0 \cdot 1$.

The form of the spectrum changes with decreasing latitude, and at the lowest frequency an intensity minimum is observed along the equator. It is shown that the observations are fully consistent with a model consisting of two components:

(i) non-thermal sources of constant spectral index

(ii) ionized hydrogen of constant temperature.

The results yield some information about the distribution of thermal and non-thermal emissivity in the galactic plane, and provide qualitative support for results which Westerhout has drawn from more limited spectral data.

I. Introduction

Below about 100 Mc/s, the galactic radio emission is mainly of non-thermal origin and has a concentration towards the galactic equator. In low latitudes the observed intensity is modified by ionized hydrogen regions which both absorb the background radiation and contribute their own component of thermal emission. They appear in absorption at very low frequencies, and in a companion paper it is shown (Shain, Komesaroff, and Higgins 1961) that individual H II regions may be distinguished as radio " dark " areas at 19·7 Mc/s.

The present paper is chiefly concerned with studying the galactic emission near the equator in directions where optical observations give no indication of H II regions, but where, nevertheless, there is an intensity minimum in the 19·7 Mc/s contours, presumably due to many H II regions beyond the range of optical observation. This is a line of investigation which Shain had intended to pursue.

If complete radio spectra for each point in the sky were available, it would be possible, subject to certain assumptions, to determine for each line of sight the magnitudes of the thermal and non-thermal components of emission and also some information about their relative distribution in depth.

At very high frequencies the optical depth of the Galaxy is generally much less than unity and the total brightness is simply the sum of the thermal and non-thermal components; because these have different spectra they can be individually determined from a number of high frequency observations. It

* Division of Radiophysics, C.S.I.R.O., University Grounds, Chippendale, N.S.W.

is only at low frequencies, for which the Galaxy is optically thick, that brightness temperatures depend on the form of the distribution in depth, and, conversely, it is only from studies of the low frequency end of the spectrum that information about the form of this distribution may be derived.

Westerhout (1958) has separated the galactic emission into thermal and non-thermal components by comparing his own 1390 Mc/s observations with those of Mills at 85 Mc/s. In effecting this separation he made the following assumptions :

(i) Within the area covered by the two surveys the non-thermal radiation is everywhere characterized by a constant spectral index,

(ii) Spectral variations are entirely due to thermal absorption in ionized hydrogen at a temperature of 10 000 °K.

Westerhout's analysis was based on only two spectral points for each direction in space ; the data were therefore inadequate to check the validity of his assumptions. The $19 \cdot 7$ Mc/s observations (Shain, Komesaroff, and Higgins 1961), having also been taken with a high resolution instrument, provide a third spectral point, and allow Westerhout's assumptions and conclusions to be tested over a range of 70 : 1 in frequency.

The main aim of the present paper is to show that for a number of directions near the equator the values of brightness temperature measured at $19 \cdot 7$ Mc/s lie well within the limits predicted from the high frequency results according to assumptions (i) and (ii) above. In addition, the low frequency observations provide a check on a further assumption that Westerhout makes, namely, that along any line of sight the ratio of non-thermal to thermal emissivity is constant. From his analysis, based on this assumption, Westerhout was led to the conclusion that ionized hydrogen is concentrated in a ring 3–4 kiloparsecs in diameter, around the galactic centre. As there is no evidence to suggest a corresponding concentration of non-thermal emission, his assumption and conclusion seem mutually contradictory. However, even at 85 Mc/s the optical depth of the Galaxy rarely exceeds $0 \cdot 3$; this means, as will be shown subsequently, that his results are fairly insensitive to the form of the assumed distribution, and therefore the contradiction does not invalidate his conclusion. At $19 \cdot 7$ Mc/s, on the other hand, optical depths are many times greater, and brightness temperatures depend quite critically on the relative disposition of the two components. Thus by comparing the three surveys we can derive additional information about the distribution in depth.

Lack of resolution, however, introduces difficulties in making the comparison. The beamwidth of the $19 \cdot 7$ Mc/s aerial is $1 \cdot 4°$, and the half-width of the intensity minimum along the equator is only about 3°. Where the observed contours are regular, it can be shown that the errors in measured equatorial temperatures due to aerial smoothing are not likely to exceed about 20%. However, the contours are often complicated by a number of " nearby " H II regions 1° or more wide ; these appear in emission at the higher frequencies as do a number of discrete non-thermal sources. The analysis has, therefore, been carried out only for areas free of strong discrete sources. There are five such areas in the overlapping sections of the three surveys, and they are the ones which have been discussed previously by Westerhout. Mathewson, Healey, and Rome are at present engaged in a 1440 Mc/s survey of the Southern Milky Way. When their results become available it may be possible to extend this type of analysis over a greater area.

II. Theory of Radio Spectra

In this section we consider the way in which the observed brightness temperature in any direction is related to the distribution of emission and absorption along the line of sight. For the moment we leave out of account the physical mechanisms underlying these processes.

Let η and $\varkappa$ be functions of spatial coordinates, and represent the total emission per unit volume and total absorption coefficient respectively. Then, if the refractive index of the medium is unity, it follows from the Rayleigh-Jeans law that the brightness temperature at a frequency f Mc/s is given by

$$T_b = \frac{c^2}{2kf^2 \times 10^{12}} \int_0^\infty \eta \exp(-\tau')\mathrm{d}s, \tag{1}$$

where $\tau' = \int \varkappa \mathrm{d}s$, c is the velocity of light *in vacuo*, k is Boltzmann's constant, and the integrals with respect to distance s are carried out along the observer's line of sight.

(a) *Non-thermal Emission*

Away from the galactic equator, brightness temperature is found to depend on frequency according to a simple power law. This is illustrated by Figure 1 in which $\log T_b$ is plotted against $\log f$ for various points in latitudes $b^{\mathrm{I}} = +4°$ and $-6°$. The brightness temperatures are taken from a number of narrow-beam surveys at the following frequencies, 19·7 Mc/s (Shain, Komesaroff, and Higgins 1961), 85 Mc/s (Hill, Slee, and Mills 1958), 240 Mc/s (Kraus and Ko 1957), 400 Mc/s (Seeger, Stumpers, and van Hurck 1960), 910 Mc/s (Denisse, Leroux, and Steinberg 1955, 1957), and 1390 Mc/s (Westerhout 1958). These results indicate that a good approximation to the spectral law is given by

$$T_b \propto f^{-2\cdot 6}. \tag{2}$$

Taking into account both the scatter in the measured values of spectral index, and also the possibility of a 20 per cent. systematic error in the measured temperatures across the frequency range, the probable error in the spectral index is about $\pm 0\cdot 1$.

Various estimates of the spectral index have been quoted in previous papers. In particular, Adgie and Smith (1956) and Costain (1960), working with scaled aerial systems, have derived the values $2\cdot 5 \pm 0\cdot 1$ and $2\cdot 37 \pm 0\cdot 04$ respectively. Both workers used broad-beam aerial systems, so that the values they quote are averages over fairly large areas of the sky. The discrepancy between the present value and Costain's could be due to a true variation with galactic latitude, with higher values of spectral index being observed near the equator than elsewhere.

Westerhout (1958) finds that the ratio of brightness temperatures at 85 and 1390 Mc/s supports a value of 2·6 but on other grounds concludes that it should be 2·7.

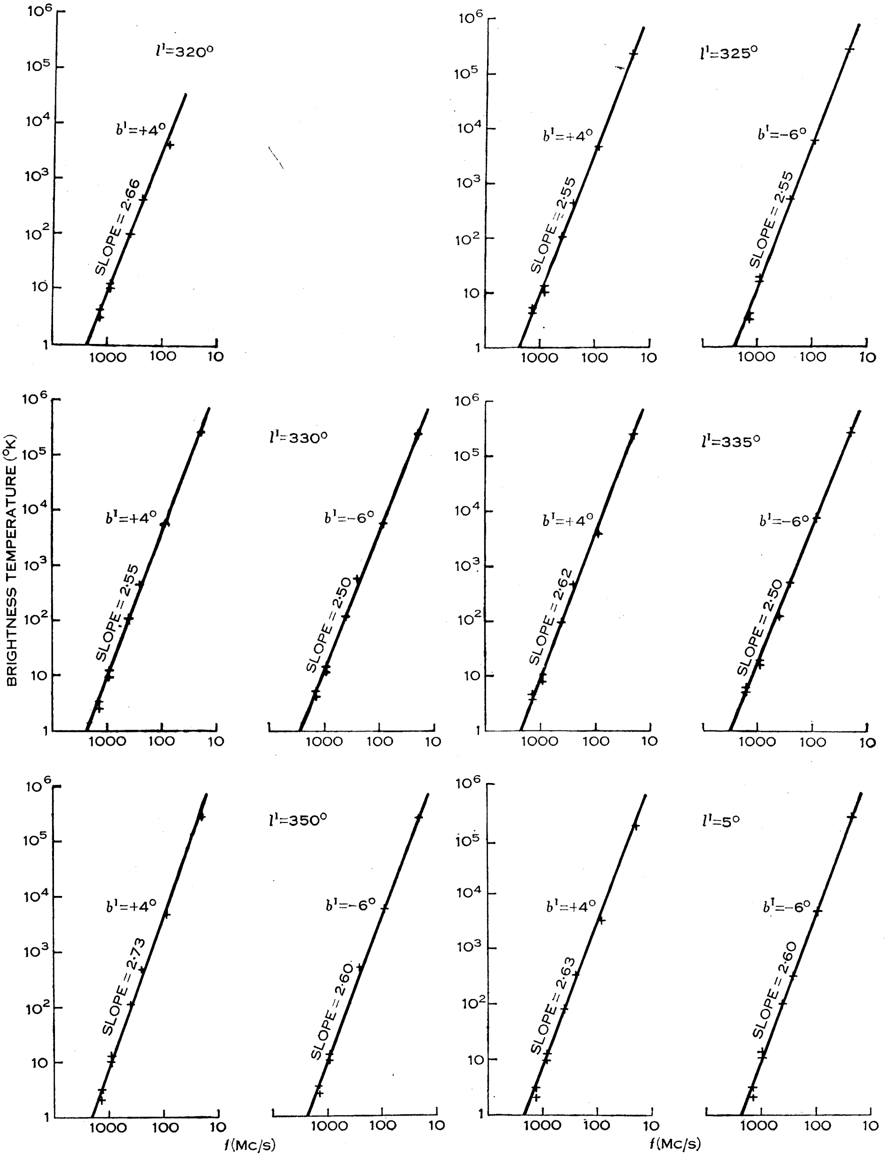

Fig. 1.—Spectra at a number of points away from the galactic equator. Brightness temperatures have been measured at the following frequencies: 19·7, 85, 250, 400, 910, and 1390 Mc/s. On each graph the Lund coordinates are given, together with an estimate of the spectral index.

The fact that the index is substantially greater than 2 indicates that the radiation is of non-thermal origin (see Piddington 1951). Equation 2 provides strong evidence that the non-thermal medium is optically thin. For, whatever the mechanism of emission, it is to be expected that η and τ' in equation (1) should depend on both frequency and direction. Therefore the most plausible assumption on which (1) and (2) can be reconciled is that

$$\tau' \ll 1.$$

(b) *Thermal Processes in Ionized Hydrogen*

Within a few degrees of the equator a simple relation like (2) no longer holds, since thermal emission and absorption in ionized hydrogen become important. Following Mills, Little, and Sheridan (1956), we assume that the electron temperature of this gas is 10 000 °K. Then, according to a recent calculation by Scheuer (1960) which takes into account the dissipative effect of both binary and multiple electron-ion collisions, the absorption coefficient per parsec is given by

$$\varkappa=(0\cdot532-0\cdot069\log_{10}f)f^{-2}N^2, \tag{3}$$

where N cm^{-3} is the electron density. Then

$$\tau'=(0\cdot532-0\cdot069\log_{10}f)f^{-2}E, \tag{4}$$

E being the "emission measure" in cm^{-6} parsec. These equations can be written in the form

$$\varkappa_f/\varkappa_{19\cdot7}=\tau'_f/\tau'_{19\cdot7}=p(f). \tag{5}$$

Numerical values of the frequency-dependent functions in (2), (3), (4), and (5) are given in Table 1.

TABLE 1

FREQUENCY-DEPENDENT TERMS USED IN THE ANALYSIS

f (Mc/s)	$\left(\frac{f}{19\cdot7}\right)^{2\cdot6}$	$\frac{\varkappa}{N^2}=\frac{\tau}{E}$	$\frac{\varkappa}{\varkappa_{19\cdot7}}=\frac{\tau}{\tau_{19\cdot7}}$ *
19·7	1	$1\cdot14\times10^{-3}$	1·0
85	45	$5\cdot52\times10^{-5}$	$4\cdot84\times10^{-2}$
1390	$6\cdot4\times10^{4}$	$1\cdot63\times10^{-7}$	$1\cdot43\times10^{-4}$

* According to the inverse-square law which is often quoted, the values are 1·0, $5\cdot4\times10^{-2}$, and $2\cdot0\times10^{-4}$.

Since the electron temperature associated with the ionized hydrogen is 10^4 °K, equation (1) may be written

$$T_b=\int_0^\infty (J+10^4\varkappa)\exp(-\tau')\mathrm{d}s. \tag{6}$$

The quantity J is related to the non-thermal brightness temperature T_n which would be observed in the absence of absorption, by the relation

$$T_n=\int_0^\infty J\,\mathrm{d}s.$$

In terms of the non-thermal volume emissivity η_n,

$$J=(c^2\eta_n/2kf^2\times10^{12}).$$

It has previously been shown that for directions a few degrees from the galactic equator, and over a wide range of longitudes, the non-thermal spectral index has a constant value of 2·6. In the subsequent argument it will be assumed that this value applies in all directions covered by the 19·7 Mc/s survey and that departures of the observed spectral law from equation (2) are due to thermal absorption. It is then convenient to introduce a " scaled up " brightness temperature $\mathscr{T}_{19\cdot7}(f)$, referred to 19·7 Mc/s, and defined by

$$\mathscr{T}_{19\cdot7}(f)=\left(\frac{f}{19\cdot7}\right)^{2\cdot6}T_b(f). \tag{7}$$

For directions in which there is no absorption, $\mathscr{T}_{19\cdot7}(f)$ is independent of frequency and equal to the measured 19·7 Mc/s brightness temperature. As we will now show, in the directions of absorbing regions, $\mathscr{T}_{19\cdot7}(f)$ increases with frequency, so that for $f>19\cdot7$,

$$T_b(19\cdot7)<\mathscr{T}_{19\cdot7}(f)\,;$$

the difference between the two quantities depends on the total optical depth of the absorbing medium, as well as its distribution in relation to the sources of non-thermal emission.

From equations (3), (4), (5), (6), (7), and the relation $\mathrm{d}s=\mathrm{d}\tau'/\varkappa$, it follows that

$$\mathscr{T}_{19\cdot7}(f)=\int_0^{\tau_{19\cdot7}}(J_{19\cdot7}/\varkappa_{19\cdot7})\exp\left[-p(f)\tau'_{19\cdot7}\right]\mathrm{d}\tau'_{19\cdot7}+(f/19\cdot7)^{2\cdot6}T_t, \tag{8}$$

where $T_t(f)$, the thermal component of brightness temperature, is given by

$$T_t(f)=10^4\{1-\exp\left[-p(f)\tau_{19\cdot7}\right]\}.$$

For very high frequencies, such that $p(f)\tau_{19\cdot7}\ll1$, we can write

$$\mathscr{T}_{19\cdot7}(f)=T_n(19\cdot7)+10^4(f/19\cdot7)^{2\cdot6}p(f)\tau_{19\cdot7}. \tag{9}$$

Since the function $p(f)$ is known, we can determine $T_n(19\cdot7)$ and $\tau_{19\cdot7}$ separately from two high frequency observations. From $\tau_{19\cdot7}$, $T_t(f)$ can then be calculated for all values of f.

(c) *Relative Distribution of the Two Components*

From what has been said, it follows that if the spectrum of the radiation is known, the integral term on the right-hand side of equation (8), which we will designate $L_{19\cdot7}(p)$, may be determined as a function of frequency. Now it may be shown that no loss of generality is incurred if an infinite upper limit replaces $\tau_{19\cdot7}$ in this integral (since $J_{19\cdot7}/\varkappa_{19\cdot7}$ is non-zero only when $\tau'_{19\cdot7}<\tau_{19\cdot7}$). Accordingly we may write

$$L_{19\cdot7}(p)=\int_0^{\infty}J_{19\cdot7}/\varkappa_{19\cdot7}\exp\left[-p(f)\tau'_{19\cdot7}\right]\mathrm{d}\tau'_{19\cdot7}.$$

This integral is a Laplace Transform. Knowing the way it varies with p, we can, by inverse transformation, determine $J_{19\cdot7}/\varkappa_{19\cdot7}$ as a function of optical depth $\tau'_{19\cdot7}$ for any line of sight. The available evidence suggests that $J_{19\cdot7}/\varkappa_{19\cdot7}$

varies quite markedly within each spiral arm, having its lowest values in absorbing regions and showing maxima where the ionized hydrogen density is low. Thus spectral studies provide, at least in principle, another approach to the elucidation of spiral structure. However, to derive detailed information about the variation of $J_{19\cdot7}/\varkappa_{19\cdot7}$ we need to know the values of $L_{19\cdot7}(p)$ down to such low frequencies (of the order of 10 Mc/s for directions near the equator) that $p(f)\tau_{19\cdot7}$ is many times greater than unity. At present there is not a sufficient number of galactic surveys of the requisite angular resolution in the relevant frequency range for this to be done in detail, but a comparison of the

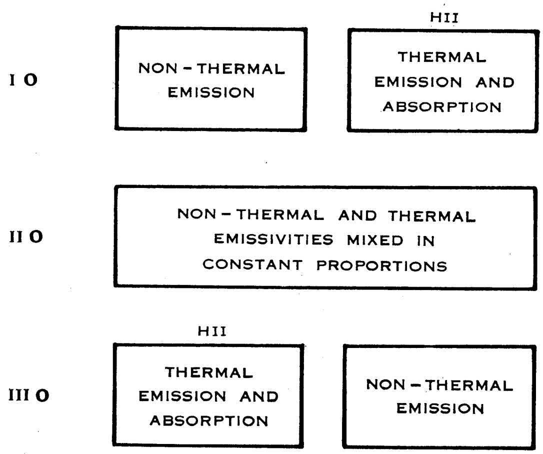

Fig. 2.—Three possible galactic models, described in the text. In each the distribution of non-thermal emission and ionized hydrogen is shown in relation to an observer at O.

$19\cdot7$ Mc/s results (Shain, Komesaroff, and Higgins 1961) with observations at higher frequencies should enable us to determine, for example, whether the mean value of $J_{19\cdot7}/\varkappa_{19\cdot7}$ in the solar neighbourhood is of the same order as for the whole Galaxy.

In Section III, the $19\cdot7$ Mc/s results are compared with those at 85 and 1390 Mc/s. Before this comparison is made, let us consider some simplified models giving the possible large-scale depth distribution of the quantity $J_{19\cdot7}/\varkappa_{19\cdot7}$. The three models to be considered are illustrated in Figure 2.

(d) *Three Simplified Galactic Models*

Model I "*Distant H* II"—It is assumed that all the non-thermal emission takes place between the observer and the ionized hydrogen. Equation (8) becomes

$$\mathscr{T}_{19\cdot7}(f)=T_n(19\cdot7)+10^4(f/19\cdot7)^{2\cdot6}\{1-\exp[-p(f)\tau_{19\cdot7}]\}. \tag{10}$$

Model II "*Perfect Mixing*".—The ratio of non-thermal to thermal emissivity does not change along the line of sight. From equation (8)

$$\mathscr{T}_{19\cdot7}(f)=\{[J_{19\cdot7}/p(f)\varkappa_{19\cdot7}]+10^4(f/19\cdot7)^{2\cdot6}\}\{1-\exp[-p(f)\tau_{19\cdot7}]\} \tag{11}$$

$$=\{[T_n(19\cdot7)/p(f)\tau_{19\cdot7}]+10^4(f/19\cdot7)^{2\cdot6}\}\{1-\exp[-p(f)\tau_{19\cdot7}]\}. \tag{12}$$

For large values of $[p(f)\tau_{19\cdot 7}]$, $\mathscr{T}_{19\cdot 7}(f)$ approaches the limiting value of

$$T_n(19\cdot 7)/p(f)\tau_{19\cdot 7}+10^4(f/19\cdot 7)^{2\cdot 6}.$$

Equation (12) has been used by Westerhout (1958) in separating the thermal and non-thermal components of brightness observed at 85 and 1390 Mc/s.

Model III "Nearby H II".—Here we assume that all the H II lies between the observer and the non-thermal medium. Equation (8) must be written

$$\mathscr{T}_{19\cdot 7}(f)=T_n(19\cdot 7)\exp[-p(f)\tau_{19\cdot 7}]+10^4(f/19\cdot 7)^{2\cdot 6}\{1-\exp[-p(f)\tau_{19\cdot 7}]\} \quad (13)$$

It is easily seen that for fixed values of $T_n(19\cdot 7)$ and $\tau_{19\cdot 7}$, the value of $\mathscr{T}_{19\cdot 7}(f)$ decreases towards the lower frequencies at a rate which is least for model I and greatest for model III. In the next section a number of galactic "crossings" are considered, and for each of these, observed values of $T_b(19\cdot 7)$ are compared with values calculated from the 85 and 1390 Mc/s observations according to each of the above models in turn.

III. Comparison of Three Radio Surveys

(a) *Five Galactic Profiles*

To apply the type of analysis just outlined we need to select areas free of strong non-thermal sources or dense localized H II regions. Suitable areas close to the equator are rare, and those which have been chosen are five previously discussed by Westerhout (1958). These are 1–2° wide and centred on $l^{\mathrm{I}}=323\cdot 5$, 332, 339, 354, and 5°. In Figure 3 the average value of $\mathscr{T}_{19\cdot 7}(f)$ is shown as a function of b^{I} for each longitude for the frequencies 19·7, 85, and 1390 Mc/s. It can be seen that for each longitude the profiles converge at high latitudes, but that towards the equator there is a relative decrease in $\mathscr{T}_{19\cdot 7}(f)$ at the lower frequencies. This is due to absorption.

In Figure 4 the observed values of $T_b(19\cdot 7)$ are again shown, together with calculated values derived from the higher frequency results according to each of the models previously described. The data on which these curves are based are given in Table 2. It is apparent that near the equator the 19·7 Mc/s results lie well within the limits given by the extreme models, I and III, and show fairly good agreement with model II. This consistency over a 70 : 1 frequency range provides excellent confirmation of the assumption on which the analysis is based, namely, that the non-thermal spectral index along the galactic plane agrees with its value measured elsewhere, and that spectral differences can be accounted for in terms of free-free transitions in ionized hydrogen. It is not to be expected that the observations should agree exactly with model II, since this is obviously an over-simplification.

In all cases the observed temperature at the equator is greater than predicted on model II. The limited resolution of the 19·7 Mc/s aerial, whose beamwidth is 1·4° (compared with 0·57° at 1390 Mc/s and 0·8° at 85 Mc/s) would tend to increase the equatorial temperatures, but from the smoothness of the profiles it can be shown that the resultant error is not likely to exceed about 20%, whereas the actual discrepancies are considerably greater; furthermore, if the effects of "nearby" H II at $l^{\mathrm{I}}=323\cdot5$, 332, and 339°, could be allowed for, the discrepancies would be greater still.

The results are therefore consistent with a galactic distribution lying between models I and II. This implies that beyond several kiloparsecs ($\tau_{19\cdot7}>1$), the ratio of thermal to non-thermal emissivity is greater than it is in the solar neighbourhood, and this is particularly the case for longitudes 323·5, 332, and 354°. According to Westerhout, the latter direction is tangential to a ring of ionized hydrogen 3–4 kiloparsecs from the galactic centre, so that the present results, although incomplete, provide qualitative support for Westerhout's conclusion.

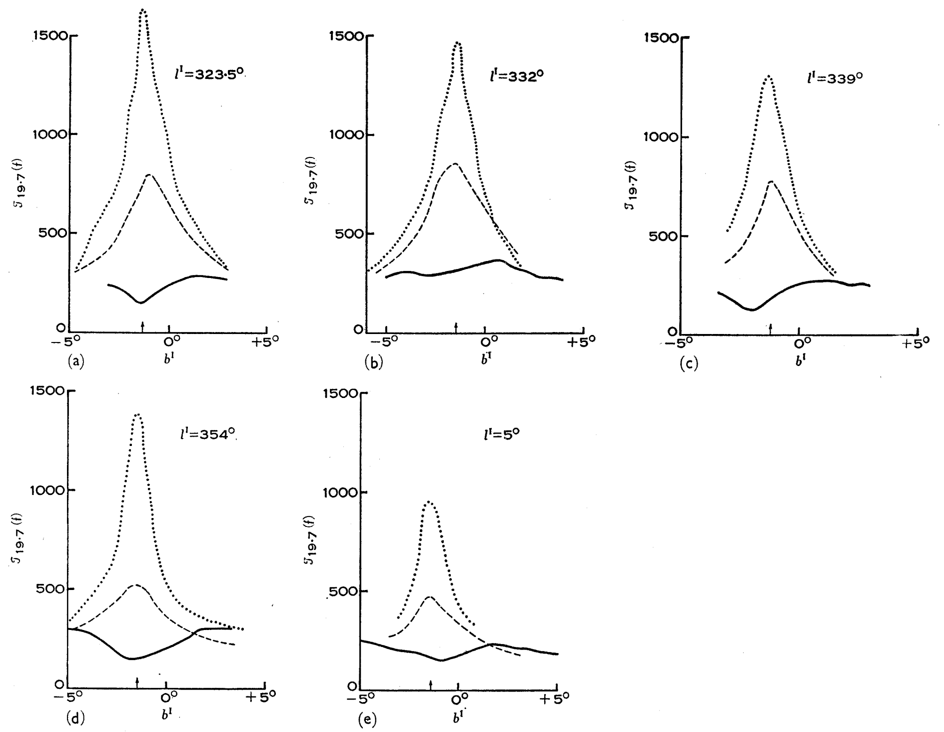

Fig. 3.—Variation of the "scaled-up" brightness temperature $\mathscr{T}_{19\cdot7}(f)$ (unit 10^3 °K), defined by $\mathscr{T}_{19\cdot7}(f)=(f/19\cdot7)^{2\cdot6}T_b$. For each of five longitudes the variation of $\mathscr{T}_{19\cdot7}(f)$ with latitude is shown for the frequencies 19·7, 85, and 1390 Mc/s : —— 19·7 Mc/s, - - - 85 Mc/s, · · · 1390 Mc/s. The equator according to the new I.A.U. system of galactic coordinates (1958 revision) is indicated by arrows.

(b) *Estimates of Emission Measures and Non-thermal Brightness Temperatures*

It has been shown that the observations are consistent with a galactic model in which in each direction the thermal and non-thermal emissivities have a roughly constant ratio. Table 2 indicates that, even if this were not the case, a separation of the 1390 and 85 Mc/s results into the two components according to this assumption, would not be seriously in error, since the limiting values of $T_n(19\cdot7)$ and $\tau_{19\cdot7}$ derived from models I and III, do not differ drastically from the model II values.

Table 2

PARAMETERS DERIVED ACCORDING TO THE THREE MODELS

(Temperature unit 10^3 °K)

l^{I}	b^{I}	$\mathscr{T}_{19\cdot7}(85)$*	$\mathscr{T}_{19\cdot7}(1390)$*	Model I			Model II			Model III		
				$\tau_{19\cdot7}$	$T_n(19\cdot7)$	$T_b(19\cdot7)$	$\tau_{19\cdot7}$	$T_n(19\cdot7)$	$T_b(19\cdot7)$	$\tau_{19\cdot7}$	$T_n(19\cdot7)$	$T_b(19\cdot7)$
323·5°	+3·2	330	300	—	—	—	—	—	—	—	—	—
	+1·6	440	510	1·1	410	420	0·9	430	280	0·9	430	190
	+0·5	570	720	2·0	530	540	1·7	550	270	1·5	580	140
	−0·4	750	1140	5·4	650	660	4·5	730	170	3·7	800	30
	−1·1	800	1550	10·0	640	650	8·3	790	110	6·7	940	10
	−1·25	780	1630	11·4	590	600	9·5	760	90	7·7	930	10
	−1·5	710	1550	11·3	520	530	9·5	680	80	7·9	830	10
	−2·0	610	1140	7·2	480	490	6·2	570	100	5·3	660	10
	−2·25	570	930	5·1	460	470	4·5	520	120	3·7	590	30
	−2·8	450	720	3·7	380	390	3·3	410	130	2·9	450	40
	−3·8	360	510	2·1	320	330	2·0	330	150	1·7	360	80
	−4·8	310	300	—	—	—	—	—	—	—	—	—
332°	+2·1	360	300	—	—	—	—	—	—	—	—	—
	+0·8	510	510	0	510	510	0	510	510	0	510	510
	+0·0	640	720	1·1	620	620	0·9	630	410	0·7	650	340
	−0·85	760	1140	5·2	670	680	4·5	730	170	3·5	820	40
	−1·2	830	1340	7·0	700	170	5·7	820	160	4·5	928	20
	−1·45	860	1470	8·3	710	720	7·0	830	130	5·4	980	10
	−1·65	860	1340	6·7	730	740	5·4	850	160	4·2	960	20
	−2·2	810	1140	4·6	720	730	3·8	790	220	3·0	870	50
	−3·0	580	720	1·9	540	550	1·6	570	280	1·4	590	160
	−4·0	430	510	1·2	400	410	1·0	420	270	1·0	420	170
	−6·0	290	300	0·2	280	280	0·2	280	260	0·2	280	240

* $\mathscr{T}_{19\cdot7}(85)$ defined as $(85/19\cdot7)^{2\cdot6}T_b(85)$ etc.

TABLE 2 (*Continued*)

l^{I}	b^{I}	$\mathscr{T}_{19\cdot7}(85)$*	$\mathscr{T}_{19\cdot7}(1390)$*	Model I			Model II			Model III		
				$\tau_{19\cdot7}$	$T_n(19\cdot7)$	$T_b(19\cdot7)$	$\tau_{19\cdot7}$	$T_n(19\cdot7)$	$T_b(19\cdot7)$	$\tau_{19\cdot7}$	$T_n(19\cdot7)$	$T_b(19\cdot7)$
339°	+2·0	260	300	0·5	260	260	0·4	260	220	0·4	260	190
	+0·5	450	510	0·8	440	450	0·7	450	320	0·7	450	250
	—0·2	570	720	2·1	520	530	1·7	560	270	1·5	580	140
	—1·1	750	1140	5·4	650	660	4·5	730	170	3·7	800	30
	—1·6	740	1300	7·7	600	610	6·5	710	120	5·2	820	20
	—2·0	610	1140	7·2	480	490	6·1	580	110	5·3	660	10
	—2·85	450	720	3·7	370	380	3·2	420	140	2·9	450	40
	—3·6	370	510	2·0	330	340	1·7	360	180	1·6	370	80
354°	+3·7	200	300	1·4	170	180	1·3	180	110	1·2	190	70
	+0·1	350	510	2·2	310	320	2·0	330	150	1·7	360	80
	—0·5	430	720	4·1	340	350	3·6	390	110	3·3	420	30
	—1·0	500	1140	8·6	350	360	7·7	440	70	6·8	520	10
	—1·5	530	1390	11·5	340	350	10·3	450	50	8·0	660	10
	—2·0	490	1140	8·7	340	350	7·9	420	60	6·9	510	10
	—2·6	430	720	4·0	350	360	3·5	400	120	3·2	420	30
	—3·4	360	510	2·1	320	330	1·8	350	160	1·7	360	80
	—5·2	280	300	0·2	280	290	0·2	280	260	0·2	280	240
5°	+0·2	310	390	1·1	290	300	1·0	300	200	0·9	300	130
	—0·6	400	600	2·9	330	340	2·6	360	140	2·4	380	50
	—1·0	440	810	5·2	330	340	4·5	400	100	4·1	420	20
	—1·55	470	950	6·6	350	360	5·9	410	80	5·2	480	10
	—1·95	430	810	5·3	320	330	4·7	380	90	4·3	410	20
	—2·2	390	600	3·0	325	340	2·7	350	130	2·5	370	40
	—2·9	300	390	1·3	270	280	1·2	280	170	1·0	300	120

* $\mathscr{T}_{19\cdot7}(85)$ defined as $(85/19\cdot7)^{2\cdot6}T_b(85)$ etc.

Westerhout (1958) has made a similar separation of the 1390 and 85 Mc/s results, based on the " perfect mixing " model, but using the following expression for optical depth,

$$\tau=(0\cdot 36/f^2)E,$$

rather than equation (4). Values of $T_n(19\cdot 7)$ and E on the equator, from the present analysis and from Westerhout's are given in Table 3.

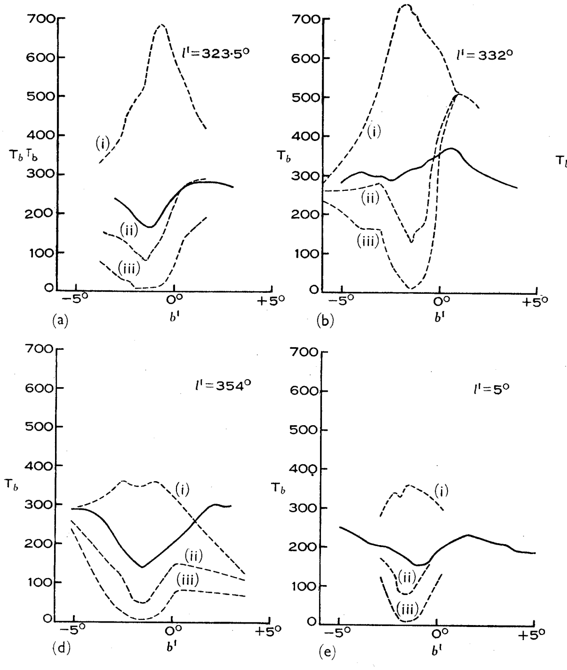

Fig. 4.—Observed (full line) and computed (dotted line) values of brightness temperature at 19·7 Mc/s (unit 10^3 °K). Curve (i) refers to model I, (ii) to model II, and (iii) to model III.

(c) *The Minima near* $l^{\rm I}=287°$ *and* $l^{\rm I}=5°$

In the companion paper (Shain, Komesaroff, and Higgins 1961) attention was drawn to the extensive " dark " areas crossing the galactic equator near longitudes 287° and 5° at 19·7 Mc/s. The optical observations indicate no large-scale H II in either direction; furthermore it can be seen from Figure 3 (*e*) that for $l^{\rm I}=5°$ the values of $\mathscr{T}_{19\cdot 7}(f)$ away from the equator agree at the three frequencies, supporting the idea that absorption is negligible. Westerhout's survey does not extend as far south as the minimum near $l^{\rm I}=287°$, but a comparison of the 85 and 19·7 Mc/s results indicates that a similar conclusion applies here also. Values of $\mathscr{T}_{19\cdot 7}(f)$ have been determined at 19·7 and 85 Mc/s for a number of longitudes at $b^{\rm I}=+3°$. In general, values at the two frequencies do not agree exactly, as we should expect them to do in the absence of absorption (part of the discrepancy is probably due to measuring error), but at $l^{\rm I}=5°$ and 287° the agreement is rather better than at most other longitudes, which supports our previous conclusion.

TABLE 3

COMPARISON OF THE PRESENT RESULTS WITH THOSE OF WESTERHOUT

l^{I}	b^{I}	Present Analysis		Westerhout's Analysis	
		E (cm^{-6} parsec)	$T_n(19 \cdot 7)$ $\times 10^{-3}$	E (cm^{-6} parsec)	$T_n(19 \cdot 7)$ $\times 10^{-3}$
323·5	−1·5	$8 \cdot 3 \times 10^3$	680	$7 \cdot 4 \times 10^3$	670
332	−1·45	$6 \cdot 1 \times 10^3$	830	$5 \cdot 3 \times 10^3$	860
339	−1·6	$5 \cdot 7 \times 10^3$	710	$4 \cdot 9 \times 10^3$	720
354	−1·5	$9 \cdot 0 \times 10^3$	450	$7 \cdot 8 \times 10^3$	460
5	−1·55	$5 \cdot 2 \times 10^3$	410	$4 \cdot 5 \times 10^3$	420

The near symmetry of the two longitudes about the galactic centre suggests that a large-scale feature of galactic structure is involved. According to the galactic model derived by Mills (1959), at these longitudes the line of sight passes between the two spiral arms nearest to the local one, towards the galactic centre. At moderate latitudes, therefore, a minimum might be expected. However, as was shown in a recent paper by Hanbury-Brown and Hazard (1960), the exact form of the distribution in longitude depends on a number of parameters which at present must be conjectional, so a more detailed interpretation will not be attempted.

IV. CONCLUSIONS

(i) About 4–5° from the equator, over a wide range of longitudes, the galactic radio spectrum is non-thermal and over a range of 70 : 1 in frequency follows the simple power law

$$T_b \propto f^{-2 \cdot 6}.$$

(ii) Nearer the equator, low frequency values of brightness temperature are consistently lower than this law predicts and, in fact, $T_b(19 \cdot 7)$ exhibits a minimum along the equator in contrast with the maximum observed at higher frequencies. This can be explained entirely in terms of thermal processes in ionized hydrogen, without invoking changes in the non-thermal spectrum.

(iii) Spectral studies provide some information about the distribution in depth of the thermal and non-thermal components. Although the present results do not give an unambiguous answer to this question, they are consistent with a model in which the ratio of non-thermal to thermal emissivity is roughly constant along any line of sight, but higher near the Sun than towards the centre of the Galaxy. On the assumption that the non-thermal emissivity is more uniformly distributed than the thermal, this is in qualitative agreement with Westerhout's conclusion that ionized hydrogen is concentrated in a ring around the galactic centre.

V. ACKNOWLEDGMENTS

The author wishes to thank Dr. J. L. Pawsey for much helpful criticism and advice while this paper was in preparation. He also thanks Mr. S. F. Smerd, who pointed out that the radio spectrum could be represented as a Laplace Transform.

VI. References

Adgie, R., and Smith, F. G. (1956).—*Observatory* **76** : 181.

Costain, C. H. (1960).—*Mon. Not. R. Astr. Soc.* **120** : 248.

Denisse, J. F., Leroux, E., and Steinberg, J. L. (1955).—*C.R. Acad. Sci., Paris* **240** : 278.

Denisse, J. F., Leroux, E., and Steinberg, J. L. (1957).—*C.R. Acad. Sci., Paris* **244** : 3030.

Hanbury-Brown, R., and Hazard, C. (1960).—*Observatory* **80** : 137.

Hill, E. R., Slee, O. B., and Mills, B. Y. (1958).—*Aust. J. Phys.* **11** : 530.

Kraus, J. D., and Ko, H. C. (1957).—Celestial radio radiation. R.F. Project 673. Sci. Rep. No. 1 Ohio.

Mills, B. Y. (1959).—" Paris Symposium on Radio Astronomy." (Ed. R. N. Bracewell.) p. 431. (Stanford Univ. Press.)

Mills, B. Y., Little, A. G., and Sheridan, K. V. (1956).—*Aust. J. Phys.* **9** : 218.

Piddington, J. H. (1951).—*Mon. Not. R. Astr. Soc.* **111** : 45.

Scheuer, P. A. G. (1960).—*Mon. Not. R. Astr. Soc.* **120** : 231.

Seeger, C. L., Stumpers, F. L. H. M., and van Hurck, N. (1960).—*Philips Tech. Rev.* **21** : 317.

Shain, C. A., Komesaroff, M. M., and Higgins, C. S. (1961).—*Aust. J. Phys.* **14** : 508.

Westerhout, G. (1958).—*Bull. Astr. Inst. Netherlds.* **14** : 215.